International Journal of Bifurcation and Chaos, Vol. 19, No. 8 (2009) 2687–2694

CONDUCTIVITY OF THE SELF-SIMILAR LORENTZ CHANNEL

FELIPE BARRA[*,†], THOMAS GILBERT[‡] and SEBASTIAN REYES[*]
[*]*Departamento de Física*
[†]*CIMAT, Facultad de Ciencias Físicas y Matemáticas, Universidad de Chile, Avenida Blanco Encalada 2008, Santiago, Chile*
[‡]*Center for Nonlinear Phenomena and Complex Systems, Université Libre de Bruxelles, CP 231, Campus Plaine, B-1050 Brussels, Belgium*

Received April 23, 2008; Revised October 2, 2008

The self-similar Lorentz billiard channel is a spatially extended deterministic dynamical system which consists of an infinite one-dimensional sequence of cells whose sizes increase monotonously according to their indices. This special geometry induces a drift of particles flowing from the small to the large scales. In this article we further explore the dynamical and statistical properties of this billiard. We derive from the ensemble average of the velocity a conductivity formula previously obtained by invoking the equality between phase-space contraction rate and the phenomenological entropy production rate. This formula is valid close to equilibrium. We also review other transport and ergodic properties of this billiard.

Keywords: Hyperbolic dynamical systems; transport properties; nonequilibrium stationary states; discrete scale invariance.

1. Introduction

Through the last twenty years, the theory of hyperbolic dynamical systems has become a cornerstone in the foundations of nonequilibrium statistical mechanics. The interest in hyperbolic models stems from relations between macroscopic features characteristic of irreversible phenomena, such as transport coefficients, and dynamical properties, such as Lyapunov exponents [Hoover, 2001; Evans & Morris, 1990; Gaspard, 1998; Dorfman, 1999].

Billiard models, have proven extremely useful in this regard [Chernov & Markarian, 2006]. The simplest example is the two-dimensional periodic Lorentz gas with finite horizon, which exhibits diffusion without a drift [Bunimovich *et al.*, 1991]. In a statistically stationary state, this model represents a mechanical system at equilibrium, with a smooth phase-space distribution. Meanwhile the process of relaxation to equilibrium itself is characterized by deterministic hydrodynamic modes of diffusion with fractal properties [Gaspard *et al.*, 2001]. One can also induce a nonequilibrium stationary state by coupling it to stochastic reservoirs of different chemical potentials at its boundaries [Gaspard, 1997]. In this case, a steady current, given according to Fick's law of diffusion, appears in the fractal nonequilibrium stationary state [Gaspard, 1998].

Whereas the previous examples of billiards are Hamiltonian systems, one can also consider dissipative periodic billiards driven out of equilibrium by the action of an external field. Thus the Gaussian iso-kinetic periodic Lorentz gas is similar to the usual periodic Lorentz gas, but for the action of a thermostated uniform external field

which bends the trajectories in the direction of the field while keeping the particle's kinetic energy constant [Hoover, 2001]. This field therefore induces a nonequilibrium stationary state to which is associated a constant drift current, given, for a small external field, by Ohm's law [Chernov *et al.*, 1993a].

A general theorem due to Wojtkowski [2000] stipulates that Gaussian iso-kinetic trajectories can be conformally mapped to the usual straight line billiard trajectories, but on a distorted geometry. Although the trajectories thus transformed do not have constant speed anymore, one can introduce, for any given trajectory, a time-reparametrization under which the speed does remain constant [Barra & Gilbert, 2007b].

Putting aside the problem of time scales and considering the dynamics of independent point-particles moving at constant speed in this new geometry, the resulting dynamics is thus conservative: particles with uniform velocities perform specular collisions on the boundary of the billiard, which consists of a sequence of asymmetric self-similar cells, scaled and put together along a one-dimensional channel. Such self-similar billiard channels were first introduced in [Barra *et al.*, 2006; Barra & Gilbert, 2007a]. They are characterized by a scaling parameter ϵ, related to the size change of the cell along the channel, and such that the usual periodic Lorentz channel is recovered when $\epsilon = 0$.

A noticeable property of these billiards concerns their long-term transport properties, characterized by a drift. Though this feature is also found in dissipative billiard models such as the Gaussian iso-kinetic Lorentz gas, the specificity of self-similar billiard channels is that the drift is the sole consequence of a geometric constraint, which does not affect the Hamiltonian character of the dynamics. In particular phase-space volumes are preserved. Furthermore, as was shown by Chernov and Dolgopyat [2008] in a recent paper, a remarkable feature of the drift in such systems is that for large enough values of the scaling parameter, the drift shows a persistent time-dependent behavior, which, on logarithmic time scales, displays periodic oscillations about its average value. In a subsequent paper [Barra *et al.*, 2007], the existence of these oscillations was demonstrated numerically, thus providing further insight into this peculiar phenomenon.

At the opposite end, for small values of the scaling parameter, time-periodic oscillations about the average drift are expected to vanish. In other words, close to equilibrium and given a fixed value of $\epsilon \ll 1$, the drift is expected to be constant. It is the value of this constant average drift that we wish to evaluate.

The aim of this paper is therefore to study the drift of particles, or mass current, in the near equilibrium regime, ($\epsilon \to 0$). We establish the results announced in [Barra & Gilbert, 2007a] and show that the current induced by the biased geometry of the channel is given by a conductivity formula, with the drift velocity being proportional to the product of the scaling parameter ϵ, which measures the departure from equilibrium, and the diffusion coefficient of the equilibrium system, i.e. the diffusion coefficient of the usual periodic Lorentz channel. This result is established by averaging the velocity with a distribution computed in the limit of small ϵ and then long time.

The paper is organized as follows. The self-similar Lorentz channel is described in Sec. 2. In Sec. 3, we show that, due to the self-similarity of the channel, it is possible to describe the dynamics of a particle in the extended channel in terms of a *pseudo* particle moving in a single (reference) cell. In Sec. 4, we review the dynamical and ergodic properties of the collision map associated with this reduced dynamics. We characterize the invariant state of the map. In Sec. 5, we summarize the main results obtained in a series of papers [Barra *et al.*, 2006; Barra & Gilbert, 2007a; Chernov & Dolgopyat, 2008; Barra *et al.*, 2007] about transport properties of self-similar billiards. Then, in Sec. 6, we obtain an expression for the ensemble average of an observable in the extended self-similar channel in terms of an average computed with the measure of the dissipative reduced dynamics in the reference cell and we apply that result to the velocity observable in the near equilibrium case. Conclusions and perspectives are offered in Sec. 7.

2. Self-Similar Lorentz Channel

Our present description of the model will be a rather compact one; we refer the reader to [Barra *et al.*, 2006; Barra *et al.*, 2007] for a detailed presentation. In order to define the self-similar channel, we have to define a reference cell. As an example, consider the reference cell of Fig. 1. In [Barra *et al.*, 2006; Barra *et al.*, 2007] two slightly different reference cells were used. They have in common many features of which we mention here the most relevant two:

1. They have two windows, Γ_L and Γ_R, whose arc-lengths are related by $\int_{\Gamma_R} ds = e^{\epsilon} \int_{\Gamma_L} ds$

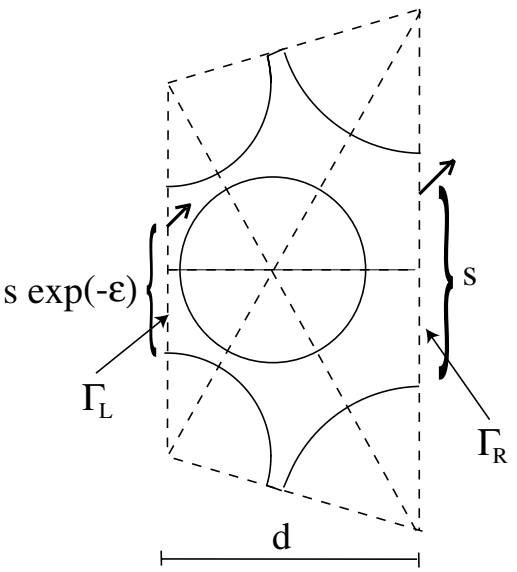

Fig. 1. Example of a reference cell and illustration of the boundary conditions.

2. If the windows are replaced by hard walls, the cell is a closed billiard with hyperbolic dynamic.

Let $\mathcal{D}_0$ denote the reference cell. The extended system is obtained from the reference cell thus defined by making a copy of it, denoted by $\mathcal{D}_1$, which we scale by a factor of $\exp(\epsilon)$ and attach to the right-hand side of the reference cell. Note that the sizes of the windows Γ_R and Γ_L are such that the left window of $\mathcal{D}_1$ coincides with the right window of $\mathcal{D}_0$. Likewise, another copy of the reference cell, this time denoted by $\mathcal{D}_{-1}$, is scaled by $\exp(-\epsilon)$ and attached to its left-hand side. By repeating this procedure, copying and scaling the right- and left-most cells and attaching these copies to the existing sequence of cells, we obtain the self-similar Lorentz channel, which consists of an infinite collection $\{\mathcal{D}_n\}_{n\in\mathbb{Z}}$ of such cells. See Fig. 2. Another property of the reference cell that we have used is that the usual Lorentz channel [Gaspard, 1998] is recovered for $\epsilon = 0$.

The self-similar structure of the channel allows us to reduce the dynamics of the *real* particle in the extended channel to the motion of a *pseudo* particle in the fundamental cell. The motion of the pseudo particle in $\mathcal{D}_0$ is associated to a reduced dynamics governed by the following rules. The pseudo particle moves as a free particle between collisions with the hard walls. At the collision it changes its direction according to the usual specular rules of elastic collisions. When the particle hits Γ_R at a point s (measured from the bottom of Γ_R) with velocity v, it instantly reappears on Γ_L at the point $se^{-\epsilon}$ (measured from the bottom of Γ_L) with velocity $ve^{-\epsilon}$. When it hits Γ_L at a point s (measured from the bottom of Γ_L) with velocity v, it reappears on Γ_R at the point se^{ϵ} (measured from the bottom of Γ_R) with velocity ve^{ϵ}. These periodic boundary conditions with rescaling of the s coordinate and the velocity are illustrated in Fig. 1. They are strictly periodic for $\epsilon = 0$.

3. The Dynamics on the Self-Similar Lorentz Channel

As we have shown, the evolution on a hierarchical billiard can be described in terms of a pseudo particle on a single cell, provided we change the speed of the particle each time it crosses the windows. In this section we give the special flow description of the reduced dynamics.

As the particle moves in the billiard its coordinates from one collision with the walls to the next are specified by the Birkhoff map [Gaspard, 1998] $\xi_n \equiv (s, w)_n \mapsto \xi_{n+1} \equiv \phi(\xi_n)$. Here the variable s represents the arc-length along the boundary of $\mathcal{D}_0$ (including the open sides) and w the sine of the angle between the outgoing velocity (always pointing to the interior of $\mathcal{D}_0$) and the normal to the cell's boundary. The map

$$\xi_{n+1} = \phi(\xi_n), \tag{1}$$

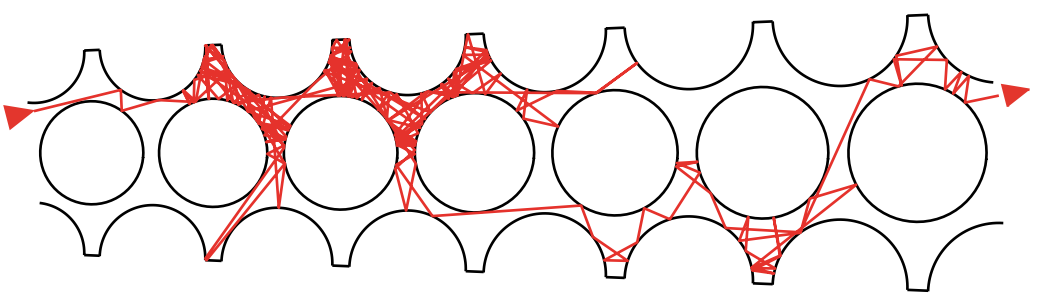

Fig. 2. Example of a self-similar Lorentz (with small ϵ) channel with a trajectory.

which determines the sequence of points visited on the boundary of the reference cell and the corresponding projection of the normalized velocity to the tangent vector, includes the boundary conditions specified at Γ_R and Γ_L. We call this map the *Poincaré map* for the pseudo particle. The area where ξ lives defines the Poincaré surface of section $\mathcal{P}$.

The speed of the pseudo particle is determined by the cell where the real particle is located. Let us introduce a new variable I_n, which takes integer values and labels the cell where the real particle is located at the nth iteration of the map. We define the jump function $a(\xi)$, such that

$$I_{n+1} = I_n + a(\xi_n), \tag{2}$$

which takes values depending on the position of the spatial coordinate s

$$a(\xi) = \begin{cases} +1, & s \in \Gamma_L, \\ -1, & s \in \Gamma_R, \\ 0 & \text{otherwise.} \end{cases}$$

The variables are related through the relation

$$I_n - I_0 = \sum_{i=1}^{n} a \circ \phi^i(\xi_0). \tag{3}$$

Observe that the *real* particle, after n reflections (n iterations of ϕ), will be exactly in the cell $\mathcal{D}_{I_n}$. Using the variable I_n we can determine the actual speed from the relation

$$v_n = \exp(-\epsilon I_n) v_0, \tag{4}$$

where v_0 is the speed in the cell $I_0 = 0$. Later, we will assume that all initial conditions are given in this cell with the same speed v_0. Every point of phase space is characterized by $\mathcal{M}_0 \ni X = [\xi, \tau, v]$ with $0 < \tau < L(\xi)$ a new variable that restores the position between collisions. Here $L(\xi)$ is the length of the trajectory issued from ξ until its intersection with the boundary of the unit cell at the next collision. The decomposition of the flow in terms of a Poincaré map and the variable τ along the trajectory issued from the Poincaré section is called a special flow [Cornfeld *et al.*, 1982].

We write this flow $\tilde{\Phi}$ explicitly. If $0 \le v_0 t + \tau < L(\xi)$, then $\tilde{\Phi}^t(\xi, \tau, v_0) = (\xi, v_0(t + (\tau/v_0)), v_0)$. At $t = (L(\xi) - \tau)/v_0$, the trajectory crosses the section $\mathcal{P}$ and we have to identify $[\xi, L(\xi), v_0] = [\phi\xi, 0, v_1]$. Further in time, and for an interval specified by $0 \le v_1(t + (\tau/v_0) - (L(\xi)/v_0)) < L(\phi\xi)$, the flow is given by $\tilde{\Phi}^t(\xi, \tau, v_0) = (\phi\xi, v_1(t + (\tau/v_0) - (L(\xi)/v_0)), v_1)$. The general case is

$$\tilde{\Phi}^t[\xi, \tau, v_0] = \left[\phi^n \xi, v_n \left(t + \frac{\tau}{v_0} - \sum_{i=0}^{n} \frac{L(\phi^i \xi)}{v_i}\right), v_n\right],$$
$$\text{if } 0 < v_n \left(t + \frac{\tau}{v_0} - \sum_{i=0}^{n-1} \frac{L(\phi^i \xi)}{v_i}\right) < L(\phi^{-n}\xi). \tag{5}$$

Note that for a set of initial conditions with the same speed v_0, the phase-space volume changes at every crossing with the windows. If a trajectory crosses Γ_R, a small volume element traveling with it changes by a factor $\exp(2\epsilon)$. Likewise, for a trajectory that crosses Γ_L, the volume element changes by $\exp(-2\epsilon)$. Thus phase-space contraction or expansion takes place whenever the particle crosses the windows. We will come back to this point in the sequel.

4. Dynamical and Ergodic Properties of the Collision Map

It is interesting to investigate the properties of the collision map for the pseudo particle associated to the continuous time dynamics described by Eq. (5)

$$(\xi, v)_n \mapsto (\xi, v)_{n+1} \equiv T(\xi_n, v_n). \tag{6}$$

From properties of the billiard geometry, this system is a single ergodic component. As we mentioned at the end of the previous section, a remarkable property of the Birkhoff map defined above is that it does not preserve phase-space volumes. Accordingly, probability measures evolve under iteration of the Frobenius–Perron operator associated to the Birkhoff map towards a unique invariant measure (i.e. a probability measure invariant under this operator) with fractal properties, characteristic of a nonequilibrium stationary state. This measure has three Lyapunov exponents, two negative and one positive, $\lambda_1 > 0 \ge \lambda_2 > \lambda_3$, and such that the phase-space contraction rate is

$$\sigma \equiv -(\lambda_1 + \lambda_2 + \lambda_3) > 0. \tag{7}$$

The second Lyapunov exponent, λ_2, is specific to the self-similar geometry of the billiard; it is due to the contraction of the v coordinate as the particle moves around the cell (equivalently to a contraction along the direction of the flow):

$$\lambda_2 = -\lim_{n\to\infty} \frac{\Delta I_n}{n} \epsilon \le 0. \tag{8}$$

where $\Delta I_n = I_n - I_0$ is the lattice displacement vector after n iterations, or winding number. If $\epsilon > 0$,

the particle moves preferentially to the right, corresponding to $\Delta I_n/n > 0$ and the other way around if $\epsilon < 0$. The symmetric case, $\epsilon = 0$, is the usual Lorentz channel, with only two nontrivial Lyapunov exponents, i.e. $\lambda_2 = 0$. We therefore see that the stationary value of v under the Birkhoff map is trivially $v_n \to v_\infty = 0$, which is to say paticles move towards the larger lattice scales, where the times separating successive collisions keep increasing and collisions become seldom.

λ_2, accounts for one half of the total phase-space contraction rate. The contraction of the vertical coordinate accounts for the other half, due to λ_1 and λ_3,

$$\lambda_1 + \lambda_3 = \lambda_2 < 0. \tag{9}$$

These two Lyapunov exponents are related to $\xi = (s, w)$.

Because the evolution of the variable ξ is independent of v, the invariant measure has a product structure

$$d^3m(\xi, v) = d^2m_1(\xi)dm_2(v) \tag{10}$$

When $\epsilon \neq 0$, we have $dm_2(v) = \delta(v)dv$ on the one hand, where δ is the Dirac delta function, and, on the other hand, the stretch and fold process

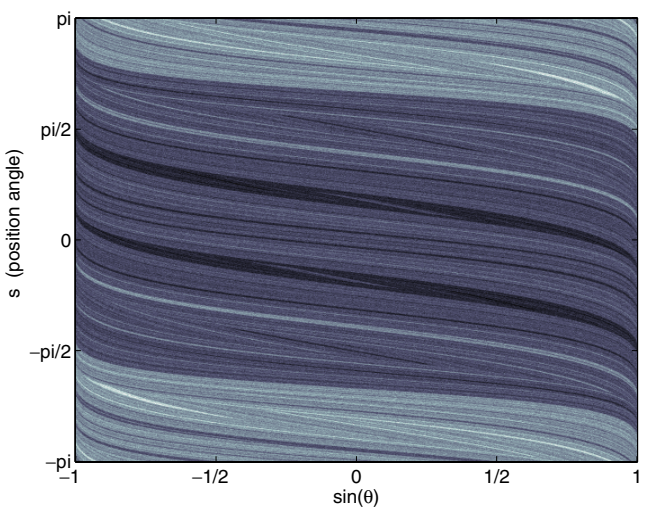

Fig. 3. Invariant measure of the Birkhoff map for the coordinates s, here restricted to the angle variable for collisions on the central disk, measured with respect to the horizontal axis as shown in Fig. 1, and $\sin\theta$, the sine of the angle between the velocity after collision and the outgoing normal to the disk. Brighter areas indicate regions of higher density. The parameter values are $R/d = 0.4336$ with R the radius of the central disc [Barra & Gilbert, 2007a] and $\exp(\epsilon) = 1.27$. The invariant measure is here computed on a grid of 500×500 cells. A total of 10^9 collision events were recorded, about 10% of which occurred on the central disk.

controlled by $\lambda_1 > 0$ and $\lambda_3 < 0$ on the plane ξ at differing rates accounts for the fractality of m_1, whose Lyapunov dimension, here defined by $1 + \lambda_1/|\lambda_3|$, is strictly between 1 and 2. A numerical computation of this fractal measure is displayed in Fig. 3. This measure m_1 is the invariant measure of the Birkhoff map ϕ.

In the following section we summarize the main statistical properties of self-similar billiards, in particular the properties of the drift. We note that the drift of real particles in the billiard chain manifests itself as a relaxation process to the invariant measure in the system with *pseudo* particles. Therefore, the invariant measure of the collision map is not directly related to the transport process of the *real* particle in the extended billiard chain. Nevertheless, we will see that in the limit $\epsilon \to 0$ it plays a role.

5. Transport Properties in Self-Similar Lorentz Channel

As we showed in [Barra *et al.*, 2006] the self-similar Lorentz channel presents some very interesting statistical properties. Among them, a mass current, i.e. a drift of particles, establishes itself in the direction of increasing cell sizes. The average velocity is expected to be constant in the regime where the scaling parameter ϵ is small. However, for large enough values of the scaling parameter, Chernov and Dolgopyat [2008] predicted the possibility that an oscillatory behavior of the drift as a function of $\ln t$ would arise. These oscillations were subsequently observed numerically and reported in [Barra *et al.*, 2007].

More precisely, let $\langle q(T)\rangle$ denote the average displacement at time T along the horizontal direction, obtained by evolving an initial distribution of points uniformly distributed in the cell $\mathcal{D}_0$ with constant speed v_0. Then, as $T \to \infty$, the ratio $\langle q(T)\rangle/T$ should behave as $f(\ln T/\epsilon)$ with f some function of period one.

For small values of ϵ, the amplitude of the oscillations is expected to vanish so that the average drift is well defined, i.e. $\langle q(T)\rangle \sim VT$. Moreover, in [Barra & Gilbert, 2007a], it was shown numerically that for $\epsilon \to 0$, this proportionality coefficient V (the average drift velocity) is related to the diffusion coefficient of the usual ($\epsilon = 0$) Lorentz channel. In the following section we show this analytically.

Let us point out, that the existence of oscillations in the drift indicates that, as time goes to infinity, the continuous time flow will not reach a

stationary time-independent state. For this reason, in the next section, we compute averages at a finite time. Then we will see in the particular case of the average velocity that if we take first the limit $\epsilon \to 0$, we can then let $t \to \infty$.

6. Averages in Self-Similar Billiards and Reduction to the Reference Cell

In the extended channel, the particle moves with constant speed v_0. Let us consider all initial conditions to be released from cell $\mathcal{D}_0$ with speed v_0 and otherwise random directions and positions. The billiard flow $\Phi^t_{v_0}$, defined on the phase space $\mathcal{M}$ of points $X = (x, y, \theta)$, is Hamiltonian and preserves phase-space volumes. Due to the symmetry of the billiard,[1] the ensemble average of an observable A,

$$\langle A\rangle_t = \int_{\mathcal{M}} dX A(X)\rho_0(\Phi^{-t}_{v_0}X), \tag{11}$$

can be expressed as

$$\langle A\rangle_t = \sum_{I=-\infty}^{\infty}\int_{\mathcal{M}_0}\mu^{2I}dY A(\mathcal{S}^I Y)\rho_0(\Phi^{-t}_{v_0}\mathcal{S}^I Y), \tag{12}$$

with $\mathcal{M}_0$ the phase space with spatial coordinates located in the reference cell, $\mu \equiv e^{\epsilon}$ and

$$\mathcal{S}Y = \mathcal{S}(x, y, \theta) = (x\mu, y\mu, \theta)\,. \tag{13}$$

For the velocity $\vec{v}(Y)$, as well as other particular observables that depend only on θ, we have $A(\mathcal{S}^I Y) = A(Y)$ and

$$\langle A\rangle_t = \int_{\mathcal{M}_0} dY A(Y)\sum_{I=-\infty}^{\infty}\mu^{2I}\rho_0(\Phi^{-t}_{v_0}\mathcal{S}^I Y). \tag{14}$$

The previous formula gives the average of A computed with respect to the measure

$$m_t(dY) = \sum_{I=-\infty}^{\infty}\mu^{2I}\rho_0(\Phi^{-t}_{v_0}\mathcal{S}^I Y)dY, \tag{15}$$

defined on $\mathcal{M}_0$. This measure is determined by the usual formula

$$m_t(dY) = \rho_t(Y)dY = \rho_0(\tilde{\Phi}^{-t}Y)\left|\frac{\partial\tilde{\Phi}^{-t}Y}{\partial Y}\right|dY, \tag{16}$$

expressed in terms of the initial distribution $m_0(dY) = \rho_0(Y)dY$, also defined on $\mathcal{M}_0$, and by the continuous time flow $\tilde{\Phi}^t$ defined on the unit cell. It follows from construction that the flow $\tilde{\Phi}^t$ is the flow described previously in Eq. (5). Using the special flow coordinates, the measure takes the form $m_t(d\xi, d\tau) = \nu_t(d\xi)(d\tau/\langle L\rangle_{\nu_t})$.

In the next section we give an explicit formula for $\nu_t(d\xi)$ in the limit of small ϵ and this will allow us to compute the average velocity

$$\langle v\rangle_t = \int_{\mathcal{P}}\nu_t(d\xi)\int_0^{L(\xi)}\frac{d\tau}{\langle L\rangle_{\nu_t}}\vec{v}(\xi) \tag{17}$$

as $\epsilon \to 0$ and $t \to \infty$. The order in which the limits are taken is important, as mentioned earlier.

6.1. *Measure $\nu_t(d\xi)$ for small values of ϵ*

Now we need to obtain $\nu_t(d\xi)$. In general, for a continuous and dissipative time flow $\dot{X} = F(X)$ with solutions $\Phi^t X_0$ for an initial condition X_0, the measure at time t,

$$d\mu_t(X) = d\mu_0(X) - \int_0^t \nabla_X\cdot F|_{\Phi^{-t'}X}d\mu_{t'}(X)dt', \tag{18}$$

is determined by the phase-space contraction rate $\nabla_X\cdot F$ [Chernov *et al.*, 1993b]. In order to apply this formula to the self-similar Lorentz channel we need to consider the phase-space contraction induced by the flow $\tilde{\Phi}^t$ on $\mathcal{M}_0$.

The reduced dynamics, which is restricted to the cell $\mathcal{D}_0$, preserves phase-space volumes, except when the trajectory crosses the boundaries Γ_L or Γ_R. Let us consider a phase-space point X and time t, such that during that time of flight, the trajectory $\{\tilde{\Phi}^\tau X\}_{0<\tau<t}$ crosses Γ_L just once. The volume change during that flight is given by

$$|\det\partial_X\tilde{\Phi}^t| = \exp(2\epsilon). \tag{19}$$

Equivalently, if X corresponds to a phase-space point that will cross once to right in time t, the volume change is

$$|\det\partial_X\tilde{\Phi}^t| = \exp(-2\epsilon). \tag{20}$$

If we consider a large time T_n such that the trajectory crosses n_1 times to the right and n_2 times to the left with $n = n_1 + n_2$ then

$$|\det\partial_X\tilde{\Phi}^{T_n}| = \exp(-2\epsilon I_n), \tag{21}$$

where $I_n = n_1 - n_2$ and $\mathcal{D}_{I_n}$ is the cell where the real particle is located at time T_n. According to the

[1] We take the origin of the (x, y) coordinates at the accumulation point of $\mathcal{D}_i$ as $i \to -\infty$. In this way, the similarity transformation $\mathcal{S}$ [see Eq. (13)] gives the symmetry of the billiard.

relation between volume change and the divergence of the flow [Gaspard, 1998], we have

$$|\det \partial_X \tilde{\Phi}^{T_n}| = \exp\left(\int_0^{T_n} \nabla_X \cdot F|_{\tilde{\Phi}^\tau X} d\tau\right) = \exp(-2\epsilon I_n). \quad (22)$$

Furthermore, because the expansion and contraction events occur only when the particle crosses Γ_L (i.e. $a(X) = -1$) or Γ_R (i.e. $a(X) = 1$) we can identify

$$\nabla_X \cdot F|_X = -2\epsilon a(X)[\delta(a(X) - 1) + \delta(a(X) + 1)]. \quad (23)$$

We now substitute Eq. (23) into Eq. (18) and compute the time integral. The Dirac deltas select points which belong to the windows $\Gamma_{L,R}$. However, due to the function a which multiplies the whole expression on the RHS of Eq. (23), we can take all the points on the Poincaré surface $\mathcal{P}$:

$$d\nu_t(\xi) = d\nu_0(\xi) + 2\epsilon \sum_{n=1}^{N_t} a(\phi^{-n}\xi) d\nu_{t_n}(\xi), \quad (24)$$

with N_t the number of times the trajectory crosses the surface and t_n the time when the trajectory is at $\phi^{-n}\xi$. In this expression, we used the fact that billiards are special flows, so that the measure at a given time t can be expressed by

$$d\mu_t(X) = d\nu_t(\xi) \frac{d\tau}{\langle L \rangle_{\nu_t}}, \quad (25)$$

with $d\nu_0(\xi)$ as the uniform measure in $\mathcal{P}$. We are interested in the limit $\epsilon \to 0$ so that for leading order we can have $\epsilon = 0$ inside the sum in Eq. (24).

6.2. *Average drift*

Now we compute the average of the velocity

$$\langle v \rangle_t = \int d\nu_t(\xi) \int_0^{L(\xi)} v(\xi, \tau) \frac{d\tau}{\langle L \rangle_{\nu_t}} = \frac{\nu_t(\Delta_\epsilon)}{\langle L \rangle_{\nu_t}}, \quad (26)$$

where

$$\Delta_\epsilon(\xi) = \int_0^{L(\xi)} v(\xi, \tau) d\tau = v_0[d\, a(\xi) + c(\phi\xi) - c(\xi)]. \quad (27)$$

The first term, proportional to $a(\xi)$ is related to the motion *along* the chain, while the second term is proportional to the difference $c(\phi\xi) - c(\xi)$ in position *inside* the cell[2] and does not contribute to the constant average drift. Thus we neglect it in the following. Therefore, transposing Eq. (24), and taking $\epsilon = 0$ inside the sum, we have that the average of a with the measure ν_t is

$$\nu_t(a) = \nu_0(a) + 2\epsilon \sum_{n=0}^{n_T} \nu_{t_n}[a(\phi_0^{-n}\xi) a(\xi)]. \quad (28)$$

Because inside the sum we take $\epsilon = 0$, we have that $\nu_{t_n}(\xi) = \nu_0(\phi_0^{-n}\xi)$, with ϕ_0 the collision map of the usual Lorentz channel. Thus the average velocity becomes

$$\langle v \rangle_t = \frac{dv_0}{\langle L \rangle_{\nu_t}} \left(\nu_0(a) + 2\epsilon \sum_{n=0}^{n_T} \nu_0[a(\xi) a(\phi_0^n \xi)]\right). \quad (29)$$

Now that we have the leading order behavior in ϵ we take $t \to \infty$ ($N_t \to \infty$) and $\langle v \rangle_t \to V$. Using the time reversal symmetry and the invariance of ν_0 under ϕ_0 (details are found in [Chernov *et al.*, 1993b] or [Gaspard, 1996]) we arrive at

$$V = \frac{2\epsilon D}{d} + o(\epsilon), \quad (30)$$

where the diffusion coefficient D of the periodic Lorentz channel appears in its discrete Green–Kubo form

$$D = \frac{d^2}{2T_{\epsilon=0}} \sum_{k=-\infty}^{\infty} \langle a(\phi^k) a \rangle_{\nu_0}, \quad (31)$$

with $T_{\epsilon=0} = \langle L(\xi) \rangle_{\nu_0} / v_0$.

6.3. *Phenomenological argument*

Equation (30) can be interpreted as an equality to leading order in ϵ between the phase-space contraction rate and minus the entropy production. As we showed in [Barra & Gilbert, 2007a], for leading order in ϵ, the winding number ΔI_n and drift velocity are equal up to dimensional factors:

$$\lim_{n\to\infty} \frac{\Delta I_n}{n} = \frac{T_\epsilon}{d} V, \quad (32)$$

where d is the reference cell's width, and T_ϵ the average time between collisions, measured in that same cell. The phase-space contraction rate [see Eqs. (7)–(9)] can therefore be expressed directly in terms of the average drift velocity:

$$\sigma = \frac{2T_\epsilon V}{d} \epsilon. \quad (33)$$

This expression can be transposed to a phase-space contraction rate per unit time in the limit $\epsilon \to 0$.

[2] $c(\xi)$ is the projection to position of ξ.

In this limit, V and ϵ both scale like ϵ, so that the lowest order contribution to σ is $\mathcal{O}(\epsilon^2)$, with T_ϵ evaluated at $\epsilon = 0$. Dividing σ by the latter defines the (dynamical) entropy production per unit time,

$$\frac{\sigma}{T_{\epsilon=0}} = \frac{2V}{d}\epsilon + o(\epsilon^2). \tag{34}$$

If we identify this with the phenomenological entropy production rate V^2/D, as e.g. in [Vollmer *et al.*, 1997], we obtain Eq. (30).

7. Conclusions

Self-similar billards are simple mechanical models of conduction in spatially extended systems with volume-preserving dynamics, whereby a geometric constraint induces a steady current. As in the conformal transformation of the Gaussian iso-kinetic Lorentz gas [Barra & Gilbert, 2007b], or the multibaker maps with energy [Tasaki & Gaspard, 1999], the essential ingredient for this behavior is the rapid increase of phase-space volumes, whose rate is here given by $\exp(\epsilon)$.

Whereas the dynamics on the extended system preserves phase-space volumes, the reduced dynamics on the reference cell contracts phase-space volumes, and thanks to this reduction we are able to express average properties of the extended system in terms of averages in the reference cell. The later can be computed by exploiting well-known properties of dissipative systems. We applied the formalism to compute the average velocity in the limit $\epsilon \to 0$ (and then $t \to \infty$) and found an expression akin to Ohm's law, with a conductivity proportional to the diffusion coefficient expressed in its Green–Kubo form. The same expression for the drift near the equilibrium regime is obtained by comparison between the phase-space contraction rate and the phenomenological entropy production.

Acknowledgments

F. Barra and S. Reyes acknowledge financial support from Fondecyt project 1060820 and Anillo ACT 15. F. Barra also acknowledges financial support from FONDAP 11980002. T. Gilbert is financially supported by the Fonds National de la Recherche Scientifique.

References

Barra, F., Gilbert, T. & Romo, M. [2006] "Drift of particles in self-similar systems and its Liouvillian interpretation," *Phys. Rev. E* **73**, 026211.

Barra, F., Chernov, N. & Gilbert, T. [2007] "Log-periodic drift oscillations in self-similar billiards," *Nonlinearity* **20**, 2539.

Barra, F. & Gilbert, T. [2007a] "Steady-state conduction in self-similar billiards," *Phys. Rev. Lett.* **98**, 130601.

Barra, F. & Gilbert, T. [2007b] "Non-equilibrium Lorentz gas on a curved space," *J. Stat. Mech.* **7**, L01003.

Bunimovich, L. A., Sinai, Ya. G. & Chernov, N. I. [1991] "Statistical properties of two-dimensional hyperbolic billiards," *Russ. Math. Surv.* **46**, 47.

Chernov, N. & Dolgopyat, D. [2008] "Particle's drift in self-similar billiards," *Ergod. Th. Dyn. Syst.* **28**, 389.

Chernov, N. I., Eyink, G. L., Lebowitz, J. L. & Sinai, Ya. G. [1993a] "Derivation of Ohm's law in a deterministic mechanical model," *Phys. Rev. Lett.* **70**, 2209.

Chernov, N. I., Eyink, G. L., Lebowitz, J. L. & Sinai, Ya. G. [1993b] "Steady state electric conductivity in the periodic Lorentz gas," *Comm. Math. Phys.* **154**, 569.

Chernov, N. I. & Markarian, R. [2006] *Chaotic Billiards*, *Math. Surveys and Monographs*, Vol. 127 (AMS, Providence, RI).

Cornfeld, I. P., Fomin, S. V. & Sinai, Ya. G. [1982] *Ergodic Theory* (Springer-Verlag, Berlin).

Dorfman, J. R. [1999] *An Introduction to Chaos in Nonequilibrium Statistical Mechanics* (Cambridge University Press, Cambridge).

Evans, D. J. & Morriss, G. P. [1990] *Statistical Mechanics of Non-Equilibrium Fluids* (Academic Press, London).

Gaspard, P. [1996] "Hydrodynamic modes as singular eigenstates of the Liouvillian dynamics: Deterministic diffusion," *Phys. Rev. E* **53**, 4379.

Gaspard, P. [1997] "Chaos and hydrodynamics," *Physica A* **240**, 54.

Gaspard, P. [1998] *Chaos, Scattering and Statistical Mechanics* (Cambridge University Press, Cambridge).

Gaspard, P., Claus, I., Gilbert, T. & Dorfman, J. R. [2001] "The fractality of the hydrodynamic modes of diffusion," *Phys. Rev. Lett.* **86**, 1506.

Hoover, W. G. [2001] *Time Reversibility, Computer Simulation, and Chaos* (World Scientific, Singapore).

Tasaki, S. & Gaspard, P. [1999] "Thermodynamic behavior of an area-preserving multibaker map with energy," *Theor. Chem. Acc.* **102**, 385.

Tasaki, S. & Gaspard, P. [2000] "Entropy production and transports in a conservative multibaker map with energy," *J. Stat. Phys.* **101**, 125.

Vollmer, J., Tél, T. & Breymann, W. [1997] "Equivalence of irreversible entropy production in driven systems: An elementary chaotic map approach," *Phys. Rev. Lett.* **79**, 2759.

Wojtkowski, M. P. [2000] "W-flows on Weyl manifolds and Gaussian thermostats," *J. Math. Pures Appl.* **79**, 953.